JOURNAL OF SOLID STATE CHEMISTRY 110, 201–207 (1994)

Infrared and Raman Spectroscopic Studies of ZrO_2 Polymorphs Doped with Y_2O_3 or CeO_2

T. Hirata,*,[1] E. Asari,† and M. Kitajima‡

*National Research Institute for Metals, 2-3-12, Nakameguro, Meguroku, Tokyo 153, Japan; †Institute of Physics, University of Tsukuba, Tennodai 1-1-1, Tsukuba, Ibaragi 305, Japan; and ‡National Research Institute for Metals, Tsukuba Laboratories, Sengen 1-2-1, Tsukuba, Ibaragi 350, Japan

Received April 12, 1993; in revised form July 6, 1993; accepted July 8, 1993

Infrared and Raman spectroscopic studies of ZrO_2 doped with Y_2O_3 (1, 2, 3, and 8 mole%) and 12 mole% CeO_2 have been done with a conventional X-ray diffraction (XRD) technique. Infrared and Raman spectra of these doped ZrO_2 polymorphs were well characterized by their unique spectral features or optical phonons. Low-temperature infrared spectroscopy also revealed that the 580 and 725 cm^{-1} modes suddenly evolve at about 123 K when the tetragonal (t)–monoclinic (m) phase transition is induced in ZrO_2–12 mole% CeO_2(Z12C); the analysis based on the oscillator strength of the B_u mode at 580 cm^{-1} revealed that the t–m phase transition occurs discontinuously with a very narrow transition width of ~2 K, whereas the oscillator strength of the E_u mode associated with the t-phase decreased toward the phase transition. It was concluded that the nonoccurrence of the t–m phase transition in tetragonal ZrO_2–3 mole% Y_2O_3(Z3Y) originates in its being less tetragonal (c/a = 1.012) than Z12C (c/a = 1.018), in the context of the dependence of the transformability on the tetragonality, as proposed by Kim. The downshift in frequency of the Raman modes for Z12C provided more evidence of a larger axial ratio for Z12C than for Z3Y through an expansion in the a-axis and the c-axis, as confirmed by XRD. It is stressed that traces of another existent phase (not predominant) at the surface and/or in the bulk can be substantiated by using infrared and Raman spectroscopic techniques at the same time as XRD. © 1994 Academic Press, Inc.

1. INTRODUCTION

There exist cubic, tetragonal, and monoclinic polymorphs of ZrO_2 at atmospheric pressure, whereas another orthorhombic polymorph of ZrO_2 is formed in a metastable state by quenching from high temperature or high pressure and is retained at room temperature (RT) in zirconia partially stabilized with magnesia (1–5).

It is well established that the stability of cubic and tetragonal polymorphs of ZrO_2 (unstable at RT) is greatly influenced by incorporating any oxide of Y_2O_3, CaO, MgO, and CeO_2 with different cation valences and ion radii, altering the force constants in the bonds (6). Hence, a large number of researches have been conducted concerning phase relations and structural phase transitions in partially stabilized ZrO_2 with dopants (7–15).

Recently, a great deal of attention has been focused on the ZrO_2–CeO_2 system, in which the tetragonal (t)–monoclinic (m) phase transition occurs autocatalytically at a grain-size-dependent temperature below zero (16–20). It has been shown that low-temperature infrared spectroscopy allows the detection of the B_u and A_u modes at 580 and 710 cm^{-1} as the t–m phase transition takes place in ZrO_2–12 mole% CeO_2 (21).

As a matter of fact, the group theoretical analysis predicts the following irreducible representations of optical phonons (for zero wave vector) for each polymorph of ZrO_2 (22, 23):

For monoclinic ZrO_2 (space group C_{2h}^5; $P2_1/c$, 4/mole/unit cell), $9A_g(R) + 9B_g(R) + 8A_u(IR) + 7B_u(IR)$;

For tetragonal ZrO_2 (space group D_{4h}^{15}; $P4_2/nmc$, 2 mole/unit cell), $A_{1g}(R) + 2B_{1g}(R) + 3E_g(R) + A_{2u}(IR) + 2E_u(IR)$;

For cubic ZrO_2 (space group O_h^5; $Fm3m$, 1 mole/unit cell), $F_{2g}(R) + F_{1u}(IR)$.

Therefore, infrared spectroscopy as well as Raman spectroscopy has been applied to phase identification and to the study of phase transitions in ZrO_2 or partially stabilized ZrO_2 with dopants (24–32), by observing infrared (IR) or Raman (R) active modes and making their assignment.

The objective of the present work is twofold. First, we do a spectroscopic study of ZrO_2 polymorphs doped with Y_2O_3 or CeO_2 by using infrared and Raman spectroscopic techniques at the same time. Second, we study the t–m phase transition in CeO_2 doped ZrO_2 in detail, trying to find out whether the t–m phase transition is possible in tetragonal ZrO_2 doped with Y_2O_3.

The present paper is organized as follows. Phase identification in the doped ZrO_2 polymorphs by X-ray diffrac-

[1] To whom correspondence should be addressed.

0022-4596/94 $6.00
Copyright © 1994 by Academic Press, Inc.
All rights of reproduction in any form reserved.

tion, infrared spectroscopy, and Raman scattering is given in Sections 3.1, 3.2, and 3.3, respectively. In Section 3.4, temperature dependence of infrared spectra of ZrO_2–12 mole% CeO_2 is measured with the intention of obtaining spectroscopic information on the t–m phase transition. Finally, the implications of the results obtained are commented upon in Section 4.

2. EXPERIMENTAL

ZrO_2 powders doped with 1 mole%, 2 mole%, and 3 mole% Y_2O_3, 8 mole% Y_2O_3, and 12 mole% CeO_2 (hereafter referred to as Z1Y or Z12C for ZrO_2 doped with 1 mole% Y_2O_3 or 12 mole% CeO_2) were prepared by Hokko Chemical Ltd. and Tosoh Corporation Inc., respectively; ZrO_2 powders (purity 99.9%) are commercially available. These powders were formed into pellets (about 1 mm in thickness and 10 mm in diameter), and then they were sintered in air at 1450°C for 4 hr and furnace cooled to RT; these pellets were used to record infrared reflectance spectra as well as Raman spectra.

Infrared reflectance spectra were measured by Fourier transform infrared spectroscopy (JEOR 100) in the frequency range 50 ~ 4000 cm^{-1}. Resolution was 2 cm^{-1} in the far infrared region and 4 cm^{-1} in the mid infrared range. For different frequency ranges, appropriate beam splitters (KBr or mylar) and a detector (triglycine sulfate (TGS)) were used, and infrared reflectance spectra are expressed as reflectance ratios of the sample to a reference (a mirror of aluminum evaporated film).

In order to measure temperature dependence of infrared reflectance spectra, temperature was varied from 298 to 77 K using a Lt-3-110 liquid transfer refrigerator system (APD Cryogenic Inc.) with heater and temperature controller (±2 K). It was possible to record low-temperature infrared spectra in the frequency range 500 ~ 4000 cm^{-1} because of a mercury–cadmium–tellurium (MCT) detector which sets a limit on measurable frequencies (>500 cm^{-1}). Raman spectra were registered with a double monochromator (JASCO TRS-660) with a spectrometric multichannel analyzer (Princeton Instruments Inc. D/SIDA 700); we used the 514.5 nm Ar^+ line for excitation with a laser power of 40 mW to collect signals from an irradiation area of the samples (about 100 μm^2). X-ray diffraction (XRD) patterns were also recorded by X-ray diffractometry (Rigaku Rad-B) with Cu$K\alpha$ radiation; we used the as-sintered pellets without any pulverization, since grinding would induce the t–m phase transition in Z12C (33), changing the originally existent phase(s) and hence their phase compositions.

3. RESULTS

3.1. *X-Ray Diffraction Patterns*

Figure 1 shows the X-ray diffraction patterns (2θ = 20 ~ 80°) of ZrO_2, Z1Y, Z2Y, Z3Y, Z8Y, and Z12C; the XRD pattern of Z12C recorded at RT after $liqN_2$-immersion is displayed as well. In Table 1, phases identified and lattice parameters determined by XRD for each sample are summarized with available crystallographic data for comparison. It is evident that the t–m phase transition would take place when Z12C was immersed into $liqN_2$; we note here that no t–m phase transition can be induced even if tetragonal Z3Y is immersed into $liqN_2$. The monoclinic phase composition v_m after the phase transition is estimated to be 72% from (36, 37)

$$v_m = [I(111)_m + (-111)_m]/[I(111)_m + I(-111)_m + I(111)_t],$$

TABLE 1
Phases Identified and Lattice Parameters Determined by XRD for ZrO_2 and Doped ZrO_2, with Available Crystallographic Data (on the Right Side)

Sample	Phase	Lattice parameters (nm)				Reference
ZrO_2	m	a = 0.5125	b = 0.5199	a = 0.5150	b = 0.5211	(5, 8, 24)
		c = 0.5291	β = 99.29°	c = 0.5317	β = 99.23°	
Z1Y	m + t(trace)	a = 0.5136	b = 0.5202	a = 0.5154	b = 0.5211	(12)
		c = 0.5295	β = 99.26°	c = 0.5318	β = 99.13°	
Z2Y	m + t(trace)	a = 0.5155	b = 0.5203	a = 0.5161	b = 0.5212	(12)
		c = 0.5307	β = 99.22°	c = 0.5322	β = 99.04°	
Z3Y	t	c = 0.5168	a = 05089	c = 0.5173	a = 0.5104	(12, 35)
		c/a = 1.012		c/a = 1.013		
Z8Y	c	a = 0.5125		a = 0.5134[a]		(8)
Z12C	t	c = 0.5221	a = 0.5127	c = 0.5222	a = 0.5125	(35)
		c/a = 1.018		c/a = 1.018		

Note. m, monocolinic; t, tetragonal; and c, cubic.
[a] The lattice parameter was extrapolated from a(Å) = 5.104 + 0.204x for $0.18 < x < 0.90$, where x is the mole fraction of $YO_{1.5}$ in ZrO_2.

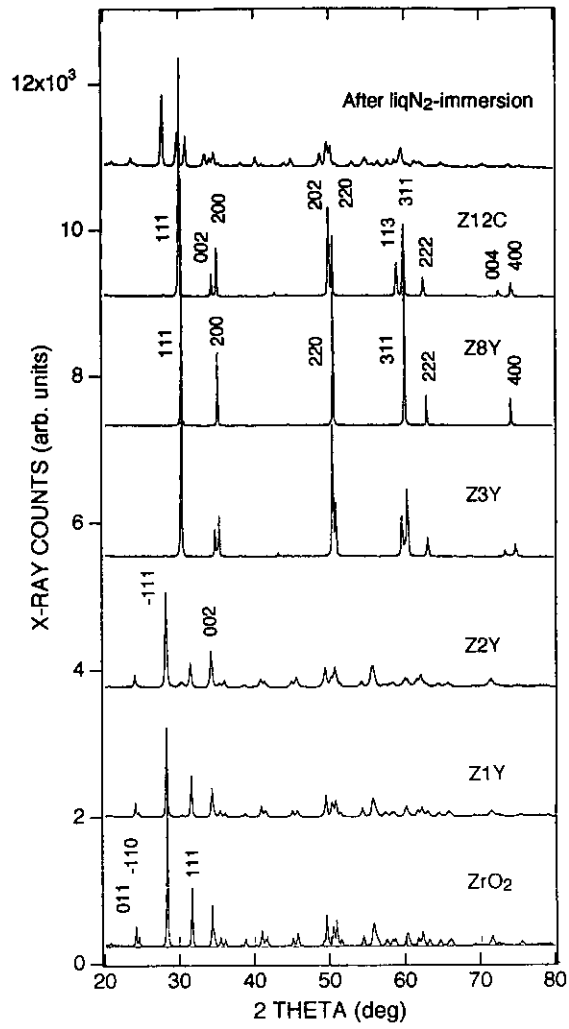

FIG. 1. XRD patterns of ZrO_2, Z1Y, Z2Y, Z3Y, Z8Y, and Z12C. The XRD pattern of Z12C recorded at room temperature after $liqN_2$ immersion is displayed as well, and these patterns are offset vertically for clarity.

where $I(111)_m$, $I(-111)_m$, and $I(111)_t$ represent the integrated intensity of the corresponding reflection for each phase. It should be noted that no complete phase transition is achieved even for prolonged immersion times (a few days) in $liqN_2$, as evidenced by some residual reflections associated with the t-phase in the XRD pattern after $liqN_2$ immersion. The grain-size-dependent temperature for the reverse m–t phase transition (19) (>200°C) in Z12C cannot account for the persistence of the t-phase reflections for the sample which only reverts to RT after $liqN_2$-immersion. No explanation for the incomplete phase transition can be given at present.

In Fig. 1, we can also notice that the scattering angles of Bragg reflections for Z12C shift downward as compared with those for Z3Y, which readily confirms that the lattice parameters for Z12C are larger than Z3Y as confirmed by XRD. Here, we note that ZrO_2 containing more than 8.0 mole% Y_2O_3 is of a single phase with the cubic structure at RT in the ZrO_2–Y_2O_3 system (8).

Also, Z1Y and Z2Y contain traces of the t-phase; note the $(111)_t$ reflection at $2\theta = 30.2°$.

3.2. *Infrared Reflectance Spectra*

Figure 2 shows the infrared reflectance spectra of ZrO_2 and Y_2O_3- or CeO_2-doped ZrO_2 in the frequency range 100 ~ 850 cm^{-1}, allowing partial overlap of the range; the infrared reflectance spectrum of Z12C after $liqN_2$-immersion is displayed as well. Among the infrared-active modes predicted by group theory, the $5A_u$ modes and the $6B_u$ modes are observed at 222 cm^{-1}, 255 cm^{-1}, 420 cm^{-1}, 445 cm^{-1}, and 730 cm^{-1}, and at 320 cm^{-1}, 350 cm^{-1}, 520 cm^{-1} (doubly degenerate), and 588 cm^{-1} (doubly degenerate), respectively, in the spectra of monoclinic ZrO_2, Z1Y, and Z2Y. These spectra are in good agreement with previous data in the literature (24, 31).

Also, an inspection of these spectra on an expanded scale enabled us to reveal a softening (≈6 cm^{-1}) of the A_u mode at 730 cm^{-1} by doping with 2 mole% Y_2O_3, which may reflect an increase in bond length(s) through the slightly expanded lattice parameters a and c by doping with Y_2O_3.

The spectra of tetragonal Z3Y and Z12C are similar to each other on the whole, exhibiting the E_u mode (broad) at 140 cm^{-1}. Another E_u mode may be recognized as a broadband over 550 ~ 650 cm^{-1}, whereas the A_u mode is not observed. A pronounced difference between the two spectra is that there exists a broadband around 320 cm^{-1} in the spectrum of Z3Y, which is assigned to the B_u mode associated with the m-phase. Hence, we can consider that the sample of Z3Y contains traces of the m-phase; this is also supported by the existence of the A_u mode at 730 cm^{-1} as a shoulder in the spectrum of Z3Y, which appears likewise with less intensity in the spectrum of Z12C.

The spectrum of cubic Z8Y is dominated by the F_{1u} mode (broad) at 628 cm^{-1}, and it is comparable to the infrared reflectance spectrum with a bay-like feature at 650 cm^{-1} in ZrO_2-12 mole% Y_2O_3 (cubic) (31). The spectrum of Z12C after $liqN_2$-immersion tends to approach the monoclinic sample spectra, indicating that the sample underwent the t–m phase transition.

Infrared spectroscopy confirmed that for tetragonal Z3Y, no t–m phase transition can be induced by $liqN_2$-immersion, and that no complete phase transition is achieved even if tetragonal Z12C is immersed for prolonged times in $liqN_2$ (independent of immersion times). No complete phase transition in Z12C is evidenced by preferential appearence of the B_u and A_u modes at lower

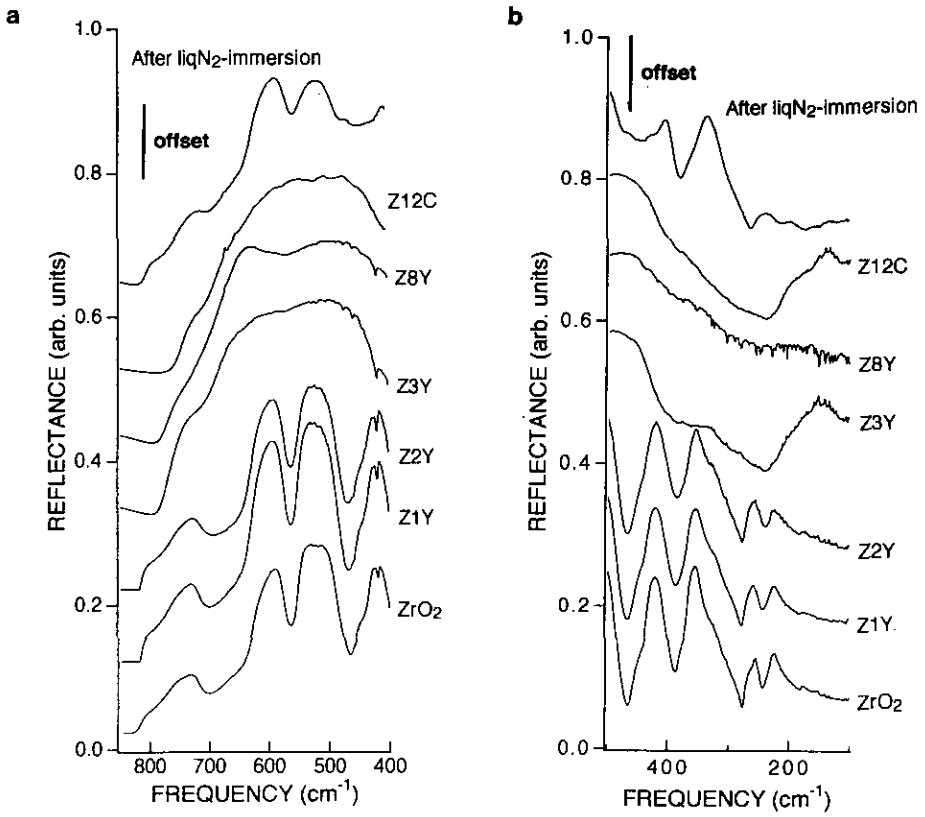

FIG. 2. Infrared reflectance spectra of ZrO_2 and Y_2O_3 or CeO_2 doped ZrO_2 in the frequency range 400–850 cm^{-1} (a) and 100–500 cm^{-1} (b), allowing partial overlap of the range; infrared reflectance spectrum of Z12C after $liqN_2$ immersion is displayed as well. Note that these spectra are offset vertically by an amount as indicated in the figure, except for the spectrum of ZrO_2.

frequencies, among the B_u modes at 320 and 350 cm^{-1}, and the A_u modes at 420 and 445 cm^{-1}, all of which are identified with the m-phase.

3.3. *Raman Spectra*

Figure 3 shows the Raman spectra of ZrO_2 and doped ZrO_2; the Raman spectrum of Z12C recorded at RT after $liqN_2$-immersion is displayed as well. In Table 2, the frequencies of the observed Raman modes and associated symmetries are tabulated, referring to the literature for their mode assignment (22–25, 29–32).

Not all 18 Raman-active modes of monoclinic ZrO_2, Z1Y, and Z2Y are observed, but their spectra are in good agreement with previously published spectra of monoclinic ZrO_2. The doping up to 2 mole% Y_2O_3 would induce disorder in monoclinic ZrO_2, which results in the diffuse A_g and B_g modes at 115 and 500 cm^{-1}. We also note that both modes B_{1g} and E_g associated with the t-phase are apparent in the Raman spectrum of Z2Y. All six Raman-active modes predicted for tetragonal Z3Y and Z12C are observed.

In addition, there exist no significant differences between the two spectra of Z3Y and Z12C, except for a downshift in frequency of the Raman modes for Z12C. The F_{2g} mode at 607 cm^{-1} dominates the Raman spectrum of cubic Z8Y. This frequency of the F_{2g} mode is higher than the calculated one (31) for Z12Y (500 cm^{-1}), but it is comparable to the experimentally observed frequency of the F_{2g} mode for stabilized cubic ZrO_2 (24).

As shown by XRD as well as infrared spectroscopy, Raman scattering also revealed that the t–m phase transition takes place in Z12C after $liqN_2$-immersion. The phase transition turned out to be incomplete as we have seen, indicating persistency of the Raman modes associated with the t-phase. The monoclinic phase composition v_m after the phase transition is estimated from the relation (29) $v_m = [I_m^{176} + I_m^{188})]/[(I_t^{152} + I_t^{247}) + (I_m^{176} + I_m^{188})]$, where I_m and I_t refer to the scattering intensity of the monoclinic or tetragonal Raman modes at frequencies shown in superscripts. We obtain the monoclinic phase composition of $v_m = 60\%$ after the t–m phase transition in Z12C, which is lower than the phase composition estimated by XRD.

3.4. *Temperature Dependence of Infrared Spectra of Z12C*

To make a spectroscopic study of low-temperature structural phase transition in Z12C, we have measured the infrared reflectance spectra of Z12C in the temperature

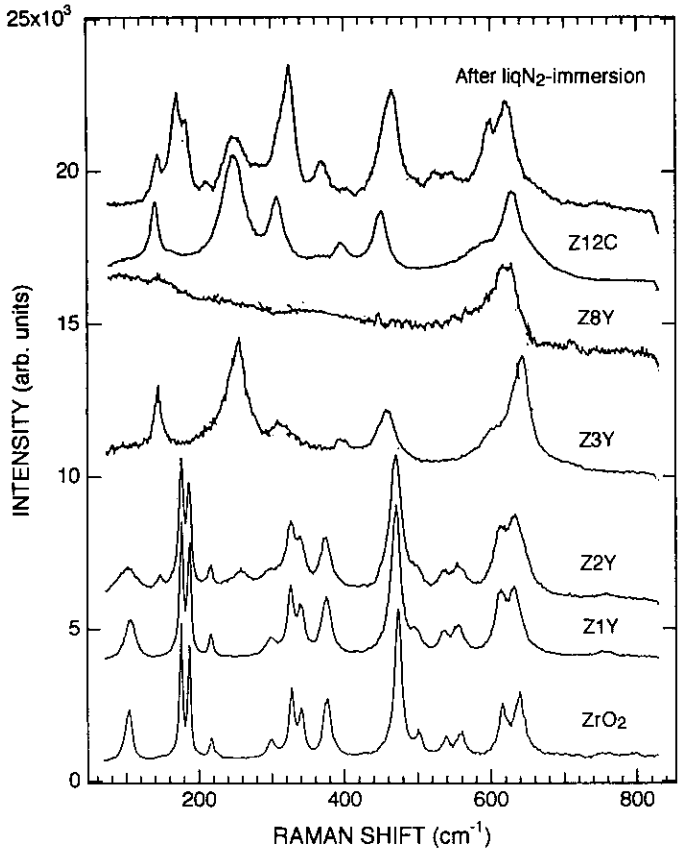

FIG. 3. Raman spectra of ZrO_2 and doped ZrO_2; Raman spectrum of Z12C recorded at room temperature after $liqN_2$ immersion is shown also.

range 298 ~ 77 K. Figure 4 displays the infrared reflectance spectra of Z12C at temperatures indicated, for demonstrating some spectral changes that are related to the t–m phase transition. No significant spectral changes are observed between 298 and 125 K.

However, only a small decrease in temperature, 2 K below 125 K, caused noticeable spectral changes. We can see that the B_u and A_u modes would evolve at 580 and 725 cm^{-1} as the t–m phase transition is induced at 123 K (21). No apparent spectral changes are observed during further cooling to 78 K. To extract any information on the phase transition from these spectral changes, the oscillator strength of the B_u mode at 580 cm^{-1} was estimated.

Figure 5 plots the estimated oscillator strength of the B_u mode as well as of the E_u mode at about 570 cm^{-1} as a function of temperature for Z12C. The oscillator strength (defined as $\int R\, dv$, with R being the reflectance) is estimated for appropriate frequency limits dv between 550 and 650 cm^{-1}.

The plot reveals the t–m phase transition at 123 K, indicating a very narrow transition width (burst-like). We can also notice that the oscillator strength of the E_u mode relevant to the t-phase tends to decrease toward the phase transition. This decreasing tendency of the E_u mode was reproducible despite several base line drawings when calculating the oscillator strength of the E_u mode. Pretransition behavior in Z12C has been found in a small decrease in full width at half maximum of the $(111)_t$ reflection with decreasing temperature (21).

TABLE 2
Frequencies (cm^{-1}) of the Raman Modes Observed in ZrO_2 or Doped ZrO_2 and Associated Symmetries

ZrO_2	Z1Y	Z2Y	Z3Y	Z8Y	Z12C	Z12C[a]
115 m A_g	117 m A_g	113 m A_g	155 s B_{1g}	607 m,b E_{2g}	148 s B_{1g}	152 s B_{1g}
183 s A_g	182 s A_g	155 [b] B_{1g}	257 s E_g		249 s E_g	176 s A_g
193 s A_g	192 s A_g	181 s A_g	305 m B_{1g}		304 s B_{1g}	188 s A_g
221 w B_g	220 w B_g	191 s A_g	410 m E_g		411 m E_g	215 w B_g
297 w A_g	295 w A_g	220 w B_g	465 s E_g		461 m E_g	247 s E_g
323 m B_g	319 m B_g	254 [b] E_g	595 [c]sh B_g		587 [c]sh B_g	319 s $B_{1g} + B_g$
334 m A_g	332 m A_g	294 w A_g	630 s A_{1g}		621 s A_{1g}	360 m B_g
392 m B_g	390 m B_g	320 m B_g				408 w E_g
476 s A_g	475 s A_g	332 m A_g				469 s $E_g + A_g$
500 w B_g	496 w B_g	389 m B_g				526 w B_g
534 w B_g	534 w B_g	475 s A_g				546 w A_g
554 w A_g	552 w A_g	500 w B_g				595 m B_g
605 w B_g	605 m B_g	532 w B_g				612 m A_g
625 m A_g	621 m A_g	549 w A_g				731 w,b B_g
726 w,b B_g	726 w,b B_g	605 m B_g				
		733 w,b B_g				

Note. w, m, and s designate weak, medium, and strong intensity, respectively; sh, shoulder; b, broad.
[a] After $liqN_2$-immersion.
[b] Tetragonal.
[c] Monoclinic.

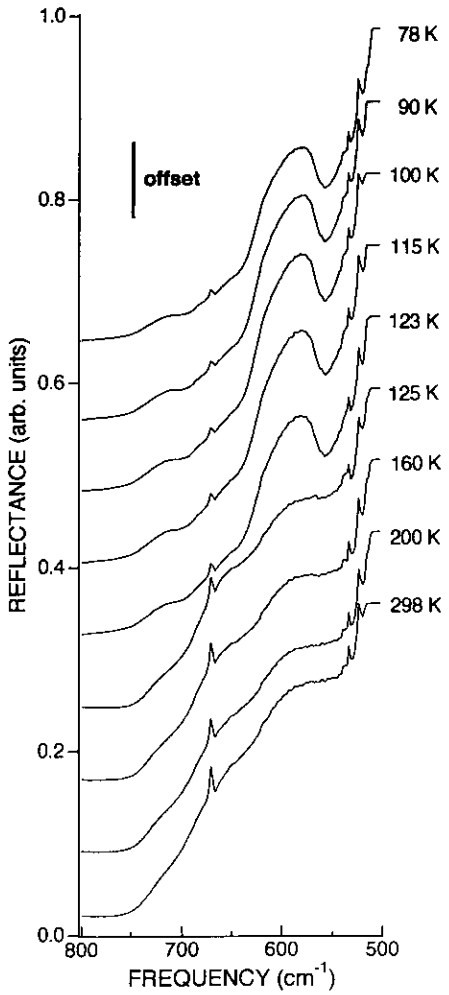

FIG. 4. Infrared reflectance spectra of Z12C at temperatures indicated, for demonstrating some pronounced spectral changes that are related to the t–m phase transition; these spectra are offset vertically by an amount as indicated in the figure, except for the spectrum at 298 K.

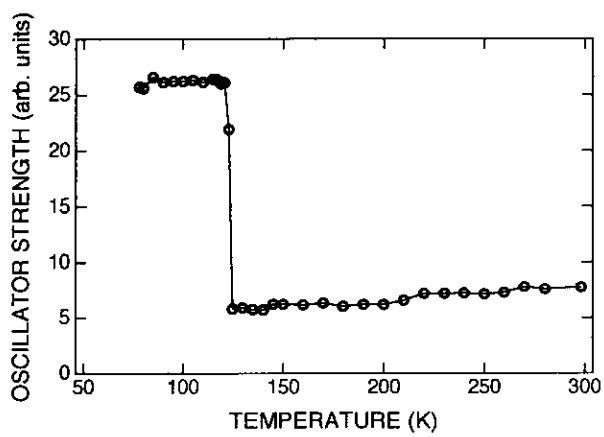

FIG. 5. Plot of the oscillator strength of the B_u mode at 580 cm^{-1} as well as the E_u mode at about 570 cm^{-1} as a function of temperature for Z12C; the oscillator strength (defined as $\int R d\nu$, with R being the reflectance) is estimated for appropriate frequency limits $d\nu$ between 550 and 650 cm^{-1}.

4. DISCUSSION

First of all, we will discuss the phase identification for doped ZrO_2. ZrO_2 doped with Y_2O_3 up to 2 mole%, as well as pure ZrO_2, is monoclinic. However, Raman scattering and XRD allowed the detection of traces of the t-phase in Z2Y, revealing the $(111)_t$ reflection at $2\theta = 30.2°$, the B_{1g} mode at 155 cm^{-1} and the E_g mode at 254 cm^{-1}, both of which are identified with the t-phase. On the other hand, there is no firm spectroscopic evidence of this phase's existence in the infrared reflectance spectrum of Z2Y.

Here, we should add that the same sample was subjected to Raman scattering, infrared spectroscopy, and XRD, to rule out the possibility that traces of other phases arise from any sample variations with respect to phase composition.

Meanwhile, the infrared spectrum of Z3Y reveals the B_u mode at 320 cm^{-1}, which is identified with the m-phase, whereas no existence of the m-phase in Z3Y is confirmed by XRD; the Raman spectra of Z3Y and Z12C also indicate the B_g mode associated with the m-phase. These differences with respect to phase identification in doped ZrO_2 may depend on different probing depths in XRD, Raman scattering, and infrared spectroscopy. XRD and Raman scattering can probe the material within a few micrometers of the surface, whereas the probing depth is somewhat larger in infrared spectroscopy. In addition, it is probable that phase compositions in doped ZrO_2 vary depending on depths from the sample surface, which may result in the different results of phase identification by the techniques with different probing depths.

Next, we discuss a reason that no t–m phase transition is possible in Z3Y, unlike in Z12C. Kim (35) has found that the tetragonality of ZrO_2-based ceramics plays a crucial role in transformability from the t-phase to the m-phase; i.e., no t–m phase transition can be induced, as the c/a ratio (tetragonality) of ZrO_2-based ceramics is closer to unity. In fact, the tetragonality of Z3Y (c/a = 1.012) is lower than the c/a = 1.018 for Z12C in the present work. Hence, no occurrence of the t–m phase transition in Z3Y can be explained in the context of the dependence of the transformability on the tetragonality. It is known that the t–m phase transition temperature in Z12C is reduced by grain refinement (18–20) and a smaller grain size may lead to a lower transition temperature below 77 K. However, we can assume that grain size has no essential role in this issue, in view of the similar grain size of 1 ~ 2 μm in both Z12C and Z3Y in the present work.

Finally, the larger c/a ratio in Z12C than in Z3Y is also supported by the downshift in frequency of the Raman modes for Z12C. This downshift in frequency correlates well with an expansion in bond lengths, i.e., through an

increase in the a-axis as well as the c-axis, as confirmed by XRD.

5. CONCLUSIONS

Infrared and Raman spectroscopic studies of Y_2O_3- or CeO_2-doped ZrO_2 have been done with a conventional X-ray diffraction technique. Infrared and Raman spectra of these doped ZrO_2 polymorphs are well characterized by their unique spectral features or optical phonons. Low-temperature infrared spectroscopy also revealed that the B_u and the A_u modes suddenly evolve at 580 and 725 cm^{-1} as the t–m phase transition is induced at about 123 K. No occurrence of the t–m phase transition in Z3Y originates in its smaller tetragonality (c/a = 1.012) than the c/a = 1.018 for Z12C, in the context of the transformability dependence on the tetragonality, as proposed by Kim. In comparison with Z3Y, the downshift in frequency of the Raman modes for Z12C, provides another piece of evidence for the larger c/a ratio in Z12C, through an expansion in the a-axis as well as the c-axis, as confirmed by XRD.

It seems likely that phase compositions in doped ZrO_2 vary, depending on depths from the sample surface, so it is stressed that traces of other (not predominant) phases at the surface and/or in the bulk can be substantiated by using infrared and Raman spectroscopic techniques at the same time as XRD.

ACKNOWLEDGMENTS

We thank Dr. Y. Muramatsu for his useful comments. We are also indebted to Mr. H. Doi for X-ray diffractometry.

REFERENCES

1. R. Suyama, T. Ashida, and S. Kume, *J. Am. Ceram. Soc.* **68**(12), C-314 (1985).
2. E. H. Kisi and C. J. Howard, *J. Am. Ceram. Soc.* **72**(9), 1757 (1989).
3. A. H. Heuer, V. Lanteri, S. C. Farmer, R. Chaim, R.-R. Lee, B. W. Kibbel, and R. M. Dickerson. *J. Mater. Sci.* **24,** 124 (1989).
4. R. J. Hill and B. E. Reichert, *J. Am. Ceram. Soc.* **73**(10), 2822 (1990).
5. C. J. Howard, E. H. Kish, R. B. Robert, and R. J. Hill, *J. Am. Ceram. Soc.* **73**(10), 2828 (1990).
6. A. N. Cormack and S. C. Parker, *J. Am. Ceram. Soc.* **73**(11), 3220 (1990).
7. R. Ruh, K. S. Mazdiyashi, P. G. Valentine, and H. O. Bielstein, *J. Am. Ceram. Soc.* **67**(7–12), C-190 (1984).
8. H. G. Scott, *J. Mater. Sci.* **10,** 1527 (1975).
9. J. R. Hellmann and V. S. Stubican, *J. Am. Ceram. Soc.* **66**(4), 260 (1988).
10. C. H. Perry, D.-W. Liu, and R. P. Ingel, *J. Am. Ceram. Soc.* **68**(8), C-184 (1985).
11. O. Ohtaka, S. Kume, T. Iwami, and K. Urabe, *J. Am. Ceram. Soc.* **71**(3), C-164 (1988).
12. H. Toraya, *J. Am. Ceram. Soc.* **72**(4), 662 (1989).
13. H. Tsubakino, R. Nozato, and M. Hamamoto, *J. Am. Ceram. Soc.* **74**(2), 440 (1991).
14. T. K. Gupta, J. H. Bechtold, R. C. Kuznicki, L. H. Ladoff, and B. R. Rossing, *J. Mater. Sci.* **12,** 2421 (1977).
15. M. T. Hernandez, J. R. Jurado, P. Duran, and J. L. G. Fierro, *J. Am. Ceram. Soc.* **74**(6), 1254 (1991).
16. N. Nakanishi and R. Shigematsu, *Mater. Trans. JIM* **30**(8), 778 (1991).
17. N. Nakanishi and T. Shigematsu, *Mater. Trans. JIM* **33**(3), 318 (1992).
18. P. E. Reyes-Morel and I. W. Chen, *J. Am. Ceram. Soc.* **71**(5), 343 (1988).
19. P. E. Reyes-Morel, J. S. Cherng, and I. W. Chen, *J. Am. Ceram. Soc.* **71**(8), 648 (1988).
20. P. F. Becher and M. V. Swain, *J. Am. Ceram. Soc.* **75**(3), 493 (1992).
21. T. Hirata, H. Zhu, T. Furbayashi, and I. Nakatani, *J. Am. Ceram. Soc.* **76**(5), 1361 (1993).
22. V. G. Keramidas and W. B. White, *J. Am. Ceram. Soc.* **57**(1), 22 (1974).
23. E. Anastassakis, B. Pupanicolaou, and I. M. A. Asher, *J. Phys. Chem. Solids* **36,** 667 (1975).
24. C. M. Phillippi and K. S. Mazdiyashi, *J. Am. Ceram. Soc.* **54**(5), 254 (1971).
25. G. A. Kourouklis and E. Liarokapis, *J. Am. Ceram. Soc.* **74**(3) 520 (1991).
26. C. S. Lim, T. R. Finlayson, F. Ninio, and J. R. Griffiths, *J. Am. Ceram. Soc.* **75**(6), 1550 (1992).
27. M. A. Krebs and R. A. Condrate, Sr., *J. Am. Ceram. Soc.* **67,** C-144 (1982).
28. T. W. Coyle, W. S. Coblenz, and B. A. Bender, *J. Am. Ceram. Soc.* **71**(2), C-88 (1988).
29. D. R. Clarke and F. Adar, *J. Am. Ceram. Soc.* **65**(6), 284 (1982).
30. K. Negita, *Acta Metall.* **37**(1), 313 (1989).
31. A. Feinberg and C. H. Perry, *J. Phys. Chem. Solids* **42,** 513 (1981).
32. M. Ishigame and T. Sakurai, *J. Am. Ceram. Soc.* **60**(7–8), 367 (1977).
33. V. E. Annamalai, T. Sornakumar, C. V. Gokularathnam, and R. Krishnamurthy, *J. Am. Ceram. Soc.* **75**(9), 2559 (1992).
34. C. J. Howard, R. J. Hill, and B. E. Reichert, *Acta Crystallogr. Sect. B* **44,** 116 (1988).
35. D. J. Kim, *J. Am. Ceram. Soc.* **73**(1), 115 (1990).
36. C. J. Howard and E. H. Kisi, *J. Am. Ceram. Soc.* **73**(10), 3096 (1990).
37. H. Toraya, M. Yoshimura, and S. Somiya, *J. Am. Ceram. Soc.* **67**(6), C-119 (1984).